DOI: https://doi.org/10.15407/rpra28.04.275
UDC 524.5, 524.6

Y.V. Vasylkivskyi, O.O. Konovalenko, and S.V. Stepkin

Institute of Radio Astronomy NAS of Ukraine
4, Mystetstv St., Kharkiv, 61002, Ukraine
E-mail: vasylkivskyi@rian.kharkov.ua

OBSERVATIONS OF DECAMETER CARBON RADIO RECOMBINATION LINES IN SEVERAL GALACTIC DIRECTIONS Part 2. ANALYSIS OF PHYSICAL CONDITIONS IN DIFFUSE CII REGIONS

Subject and Purpose. *In Part 2 of the current paper, we seek to analyze the observational results of decameter carbon radio recombination lines (RRLs) detected near the frequency 26 MHz through the UTR-2 radio telescope towards the S140 emission nebula and the GSH 139-03-69 super shell. These lines have proven themselves as a highly effective tool for cold, rarefied interstellar medium (ISM) diagnostics. The aim is to determine an association of line-forming regions (CII regions) with other ISM components and study physical conditions (electron temperature T_e and electron density N_e) in these regions.*

Methods and Methodology. *By iterative comparison of detected and modeled integral intensities of decameter carbon RRLs, we determine physical state ranges where recorded experimental data best fit the model values for various combinations of T_e, N_e, and path lengths s.*

Results. *It has been found that the characteristics of the detected decameter carbon RRLs are consistent with the higher-frequency data for both the S140 line of sight and other Galactic plane directions, including the GSH 139-03-69 direction. Ranges of physical conditions where recorded data and model values are in the best agreement have been determined, being $T_e = 50 \div 100$ K, $N_e = 0.01$ cm^{-3}, and $s = 10$ pc — for the S140 nebula direction and its vicinity and, also, $T_e = 50 \div 100$ K, $N_e = 0.01$ cm^{-3}, and $s = 5 \div 7$ pc — for the GSH 139-03-69 super shell direction.*

Conclusions. *The obtained results indicate that the detected decameter carbon RRLs originate from CII regions associated with clouds of diffuse neutral hydrogen HI in the Galactic plane. The lines are seen against a background Galactic radio emission whose brightness temperature increases as frequency decreases.*

Keywords: *electron density, electron temperature, interstellar medium, ionized carbon, medium model, radio recombination lines, CII region.*

Citation: Vasylkivskyi, Y.V., Konovalenko, O.O., Stepkin, S.V., 2023. Observations of decameter carbon radio recombination lines in several Galactic directions. Part 2. Analysis of physical conditions in diffuse CII regions. *Radio Phys. Radio Astron.*, **28**(4), pp. 275—286. https://doi.org/10.15407/rpra28.04.275

Цитування: Васильківський Є.В., Коноваленко О.О., Степкін С.В. Спостереження декаметрових рекомбінаційних радіоліній вуглецю в деяких напрямках Галактики. Частина 2. Аналіз фізичних умов у дифузних CII-областях. *Радіофізика і радіоастрономія*. 2023. Т. 28. № 4. С. 275—286. https://doi.org/10.15407/rpra28.04.275

Introduction

Part 1 [1] of the current paper presents observational results of decameter carbon radio recombination lines (RRLs) detected near the frequency 26 MHz in the S140 emission nebula and the GSH 139-03-69 super shell directions through the UTR-2 radio telescope. Discovered more than forty-five years ago [2], decameter RRLs have become one of the most effective diagnostic tools for the cold, rarefied interstellar medium (ISM) [3—5]. By studying decameter RRLs, one gains electron temperature, T_e, electron density, N_e, emission measure, pressure, mechanisms of ionization and recombination in tenuous interstellar plasma regions located away from strong ionization sources, such as stars or HII regions. The main source of ionization is far-ultraviolet (FUV) photons with wavelengths of 912 Å $< \lambda <$ 1 100 Å that flood out from HII regions in the Galactic plane.

It should be noted that at low densities, the interstellar gas gets out of local thermodynamic equilibrium (LTE) [3]. The populations of highly excited levels in the non-LTE case are characterized by the departure coefficient, b_n, which represents the ratio of the actual population at a given quantum level n to the LTE population. At $T_e \sim 100$ K, the highly excited levels in carbon atoms can be populated under the low-temperature dielectronic-like recombination process, which may considerably change line intensities [6].

The objects of the present research are the Galactic plane medium lying in the directions of the S140 emission nebula and of the GSH 139-03-69 super shell.

The S140 nebula direction is remarkable for the S140 location at the edge of the L1204 molecular cloud. The S140/L1204 line of sight has been explored in RRLs at different frequencies. The observations [7] of high-frequency carbon recombination lines C142α and C166α indirectly suggest that the line-forming region (ionized carbon zone, or CII region) exists towards the S140/L1204 complex. Studies [8] of the H165α, H166α, C165α, and C166α recombination lines conducted near the frequency 1 420 MHz towards the S140/L1204 complex through the use of the 100-meter Effelsberg radio telescope show that the physical conditions in the CII region are $T_e \sim 75$ K and $N_e \sim 0.5$ cm^{-3}.

Also, the S140 line of sight was investigated in decameter carbon RRLs. Low-frequency carbon line C640α near 25 MHz in the S140 direction was first detected using the UTR-2 radio telescope [9]. The observed relative line intensities were estimated to be $10 \pm 3 \cdot 10^{-4}$ and $5 \pm 2 \cdot 10^{-4}$ for "North-South" and "West-East" arrays of the UTR-2, respectively, with the RRL radial velocities being, respectively, -6 ± 17 and -36 ± 17 km/s. Based on the obtained line width 8 ± 2 kHz (or 96 ± 24 km/s when measured in more convenient velocity units independent of frequency changes), the authors [9] obtained the upper limit $N_e \leq 1$ cm^{-3} of the electron density and found that $T_e \geq 20$ K. The linear and angular dimensions of CII region responsible for the low-frequency line formation towards the S140 were estimated to be, respectively, 2÷6 pc and 7′÷20′ at about a 1 kpc distance to the S140. Notice they did not consider the mechanism of the highly-excited level population via the low-temperature dielectronic-like recombination in their analysis.

An attempt was made [10] to detect C540α line in the S140 direction near 42 MHz through the DKR-1000 radio telescope. It was not successful despite the fact that C540α line was expected to have a higher intensity than decameter C640α line. However, the authors determined the threshold ($\leq 3.6 \cdot 10^{-4}$) of RRL intensity detection at meter wavelengths. They also explain a rather large line width of C640α in [9], suggesting that the main line-broadening contributor is high-speed turbulent motions in the ISM rather than collisions between Rydberg atoms and electrons. That large line width is not consistent with high-frequency carbon RRL widths (approximately 2÷5 km/s). Work [10] suggests that CII region of the observed decameter carbon RRL formation in the S140 direction is not associated with the S140 nebula itself. A comparison [10] between the observational data of C640α and HI lines shows their good agreement, with the maxima of both lines corresponding to the radial velocities centered at about 0 km/s. In addition, work [10] supposes that decameter RRLs in the S140 direction are formed in multiple diffuse HI clouds located in the line of sight. The typical parameters of the clouds are $N_H = 6 \div 20$ cm^{-3}, $N_e \sim 0.02$ cm^{-3}, and $T_e = 60 \div 80$ K, and carbon in them is fully ionized by FUV radiation, 912 Å $< \lambda <$ 1 100 Å. Also, decameter carbon RRL observations [11] made in the S140 direction due to the UTR-2 radio telescope combined with a 4096-channel digital correlator show that the considered CII region apparently

exceeds the S140 nebula in angular size and is not spatially associated with it.

The GSH 139-03-69 super shell direction is also worth examining in low-frequency RRLs. As just mentioned, "classical" HI clouds, are characterized by $T_e = 60 \div 80$ K, $N_e \sim 0.02$ cm^{-3}, and $N_H = 6 \div 20$ cm^{-3} and have long been intensively studied in HI line. Among numerous investigations of the Galactic plane in HI line, the Leiden/Argentina/Bonn (LAB) Survey [12] is considered the most sensitive with the most extensive coverage. Apart from "classical" HI clouds, there are also HI clouds composed of even cooler gas. They are normally smaller than the "classical" ones and easier to explore against bright discrete sources. Their study in HI self-absorption line (absorption of the cold cloud component in warmer HI radiation of the Galactic background) against Galactic background is rather difficult.

However, there are still larger reservoirs of cold HI in the Galaxy. They not only surpass the "classical" HI clouds but also molecular clouds and even molecular cloud complexes. An example is the GSH 139-03-69 super shell located in the Galactic plane. The GSH 139-03-69 is 9 kpc away from the Sun and 16 kpc from the Galactic center and is as large as 2.8 kpc × 1.6 kpc. Its northern edge of the size $l \times b = \sim 15° \times 1°$ was studied in HI self-absorption line through the Synthesis Telescope of the Dominion Radio Astrophysical Observatory [13]. An immense volume of cold atomic hydrogen with a large optical depth ($\tau \approx 1$) and low brightness temperatures of the shell ($\sim 10 \div 20$ K) and of the background HI gas ($\sim 15 \div 40$ K) was discovered. The given estimates represent temperature thresholds in the GSH 139-03-69 direction. In fact, they can be even lower, but not under 2.7 K, the temperature of the "relict" microwave background. The range of radial velocities obtained from observations of self-absorption HI line is within –87 to –59 km/s. The mass of this GSH 139-03-69 super shell is $(1.9 \cdot 10^7) \times M_\odot$, or 48 masses of the "classical" diffuse HI clouds. The upper limit of the column density comes to be $5 \cdot 10^{19}$ cm^{-2}. Atomic hydrogen at these low temperatures is quite rarely observed in the Galaxy. The analysis in [13] shows that the existence of such a large volume of cold HI gas in the ISM contradicts the prevailing view that the cold gas mainly resides in molecular clouds. So, the results from [13] encourage further research into such volumes of sufficiently cold atomic gas against Galactic background radio emission. Although the exact mechanism of this super shell formation is not available yet, a significant place the objects of this sort fill in multiphase ISM structure is evident.

Part 2 of the current paper is devoted to the analysis of decameter carbon RRL observations through the UTR-2 radio telescope and is organized as follows. Its Section 1 considers available models of CII regions. Sections 2 and 3 discuss physical conditions in CII regions towards the S140 and the GSH 139-03-69, respectively, with admissible T_e and N_e ranges, where observational and modeling data come closest. Conclusions follow in the last Section.

1. Models of CII regions

There are two well-known types of CII regions. One is often called the "classical" CII region and is directly related to HII regions, with the ionization occurring through radiation from stars within HII region. This type of CII regions presumably forms high-frequency carbon RRLs. The other type is called the "diffuse" CII region. It is associated with clouds of neutral hydrogen HI, where carbon is ionized by FUV photons, 912 Å $< \lambda <$ 1 100 Å, emanating from HII regions. The diffuse CII regions produce low-frequency carbon RRLs [3, 4].

Among various models [14—22] developed for the diffuse CII regions, the "cold" and "warm" medium models are highlighted. The "cold" medium model is for $T_e \sim 20$ K and $N_e \sim 0.3$ cm^{-3}, the RRLs are associated with the molecular hydrogen component of the ISM [14, 16, 19]. The "warm" medium model is for $T_e \sim 35 \div 75$ K and $N_e \sim 0.05 \div 0.1$ cm^{-3}, the RRLs are associated with omnipresent diffuse HI gas [15, 17, 18, 20]. The best agreement between theoretical predictions and recorded data is observed in a wide range of frequencies for the Cas A models. In support, a good agreement with the "warm" model is shown in [20] for the medium physical conditions $T_e \sim 75$ K and $N_e \sim 0.02$ cm^{-3}. The highly-excited levels in this case are populated under the low-temperature dielectronic-like recombination mechanism [6].

A still better agreement between experimental results and the "warm" model predictions was caught in low-frequency carbon RRL observations towards other Galactic directions. Work [23] suggests that low-frequency carbon RRLs in Galactic plane directions originate from diffuse HI clouds in the line of sight. The analysis made in [11] suggests that CII re-

gion that produces decameter lines is not associated with the S140 nebula itself. Apparently, decameter lines in the S140 direction form in the diffuse HI clouds lying in the line of sight. On the other hand, work [24] proposes that depending on its size, CII region can be associated both with the diffuse neutral hydrogen HI cloud (about 2° in size) at higher temperatures and lower densities ($T_e \sim 60 \div 300$ K and $N_e \sim 0.03 \div 0.05$ cm^{-3}) and with the photodissociation region on the surface of the molecular clouds (more than 4° in size) with lower temperatures and higher densities ($T_e \sim 20 \div 40$ K and $N_e \sim 0.1 \div 0.3$ cm^{-3}).

In light of all the above, it is important to carry out decameter radio observations of carbon recombination lines in different Galactic directions. The refinement of physical parameters, the medium model improvements, and the size estimation of CII regions are essential for subsequent astrophysical analysis. As to the GSH 139-03-69 super shell direction, the observations of decameter RRLs are not only a good way to probe the physical conditions in CII regions but also to confirm the existence of such giant extremely cold HI gas complexes in the Galactic plane and to more augment our understanding of their structure, evolution and kinematic parameters.

2. Analysis of physical conditions in the S140 line of sight and its vicinity

The results obtained in [9] were interpreted in the framework of the available ISM models. As was already mentioned, with the authors' supposition [9] of low electron temperatures (much less than 100 K), the level population mechanism through the low-temperature dielectronic-like recombination whose efficiency is at its highest at around 100 K was not considered [9].

According to [10, 23], the Doppler broadening makes the main contribution to low-frequency carbon RRL widths observed both in the S140 direction and in other Galactic plane directions. The line widths towards the S140 and its vicinity in our study and in work [11] are much smaller than those in [9]. Comparing the line widths obtained in our work with the line widths in other directions of the Galactic plane at 76 and 34.5 MHz [23, 24] shows that in terms of radial velocities, these line widths are very close. There is no significant line broadening as frequency decreases, which indicates the Doppler broadening mechanism dominance of. A large difference (several times the value) from the line widths in [9] can be attributed, on the one hand, to a better sensitivity of our digital correlator distinguished by a wider bandwidth and a larger number of simultaneously observed transitions and, on the other, to the improved procedure of profile fitting.

In work [9], the lines with a relative intensity of about $10 \pm 3 \cdot 10^{-4}$ against the continuum were ob-

Table 1. **Integral intensities calculated from Equation (1) for six electron temperature and electron density combinations associated with three path lengths and two departure coefficient values**

T_e, K	N_e, cm^{-3}	s, pc	$b_n\beta_n$	Model I_L, s^{-1}
50	0.01	5	13 (from [6])	–0.7353
			9 (from [25])	–0.5091
		7	13 (from [6])	–1.029
			9 (from [25])	–0.7127
		10	13 (from [6])	–1.47
			9 (from [25])	–1.01823
	0.1	5	13 (from [6])	–73.53
			3 (from [25])	–16.97
		7	13 (from [6])	–102.95
			3 (from [25])	–23.75
		10	13 (from [6])	–147.077
			3 (from [25])	–33.94
	1	5	8 (from [6])	–4525.47
			1 (from [25])	–565.68
		7	8 (from [6])	–6335.6
			1 (from [25])	–791.958
		10	8 (from [6])	–9050.95
			1 (from [25])	–1131.36
100	0.01	5	75 (from [6])	–0.75
			8 (from [25])	–0.08
		7	75 (from [6])	–1.05
			8 (from [25])	–0.112
		10	75 (from [6])	–1.5
			8 (from [25])	–0.16
	0.1	5	70 (from [6])	–70
			6 (from [25])	–6
		7	70 (from [6])	–98
			6 (from [25])	–8.4
		10	70 (from [6])	–140
			6 (from [25])	–12
	1	5	28 (from [6])	–2800
			1 (from [25])	–100
		7	28 (from [6])	–3920
			1 (from [25])	–140
		10	28 (from [6])	–5600
			1 (from [25])	–200

served using the "North-South" UTR-2 array. The relative intensity in the present study is slightly lower, which is attributable to peculiarities of the baseline extraction procedures.

Notice when the continuum is lacking a powerful source whose brightness temperature exceeds the brightness temperature of the Galactic background, the relative line intensity observed does not correspond to the actual intensity in the ISM. In this case, correction factors should be introduced to take into account the angular size ratio of the studied CII region and the radio telescope beam and the background and foreground brightness temperatures of the CII region. Not knowing spatial dimensions of the CII region and its background and foreground brightness temperatures prevents an exact estimation of real intensities. Yet, it is possible to use the integral line intensities, I_L, that directly depend on the ISM physical conditions, namely the electron temperature and the electron density, as follows [4]

$$I_L = \int_{\nu} \frac{\Delta T_L}{T_C} d\nu \approx -2 \cdot 10^6 \frac{N_e^2 s}{T_e^{5/2}} b_n \beta_n, \qquad (1)$$

where $\Delta T_L / T_C$ is the relative line intensity, s is the path length in pc, b_n is the coefficient of departure from LTE state, and β_n is the stimulated emission factor.

The integral line intensities were determined from the experimentally obtained spectra (Table 2 in [1]). These observational values were used for comparison with the model values obtained by the iterative substitution of various T_e and N_e combinations into Equation (1) (Table 1). For the analysis, the six following T_e and N_e combinations were taken: (1) T_e = 50 K, N_e = 0.01 cm^{-3}, (2) T_e = 50 K, N_e = 0.1 cm^{-3}, (3) T_e = 50 K, N_e = 1 cm^{-3}, (4) T_e = 100 K, N_e = 0.01 cm^{-3}, (5) T_e = 100 K, N_e = 0.1 cm^{-3}, and (6) T_e = 100 K, N_e = 1 cm^{-3}. The analysis is similar to that in [11] but compounded by the addition of the path length s equal to 5, 7, or 10 pc to each of the six T_e and N_e combinations. Also, the $b_n\beta_n$ values taken from [6] are used along with those from the more recent paper [25] which adopts a more rigorous method of the statistical equilibrium equation calculation and more adequately takes into account collision rates.

The results of the comparative analysis between observational and model values for the S140 line of sight are listed in Table 2 and plotted on graphs in Fig. 1. The best agreement takes place for combinations (1) and (4) with the path length s = 10 pc and $b_n\beta_n$ taken from [6] and, also, for combination (1) with $b_n\beta_n$ from [25] and, s = 10 pc. The directions of S140 neighborhoods received the same analysis, see Table 2 and Figs 2 and 3. For the G105.15+2.8 direction, combinations (1) and (4) with s = 10 pc and

Table 2. **Model combinations of physical conditions which best suit the observational data**

Direction	Observed I_L, s^{-1}	Best suited model I_L, s^{-1}	Best suited T_e, K	Best suited N_e, cm^{-3}	Best suited s, pc	Best suited $b_n\beta_n$
S140	–1.54	–1.47	50	0.01	10	13 (from [6])
		–1.5	100	0.01	10	75 (from [6])
		–1.01823	50	0.01	10	9 (from [25])
G105.15+2.8	–2.93	–1.47	50	0.01	10	13 (from [6])
		–1.5	100	0.01	10	75 (from [6])
		–1.01823	50	0.01	10	9 (from [25])
G108.48+7.83	–1.04	–1.029	50	0.01	7	13 (from [6])
		–1.05	100	0.01	7	75 (from [6])
		–1.01823	50	0.01	10	9 (from [25])
G140+00	–1.07	–1.029	50	0.01	7	13 (from [6])
		–1.05	100	0.01	7	75 (from [6])
		–1.01823	50	0.01	10	9 (from [25])
GSH 139–03–69	–0.78	–0.7353	50	0.01	5	13 (from [6])
		–0.75	100	0.01	5	75 (from [6])
		–0.7127	50	0.01	7	9 (from [25])
G145+00	–0.95	–1.029	50	0.01	7	13 (from [6])
		–1.05	100	0.01	7	75 (from [6])
		–1.01823	50	0.01	10	9 (from [25])

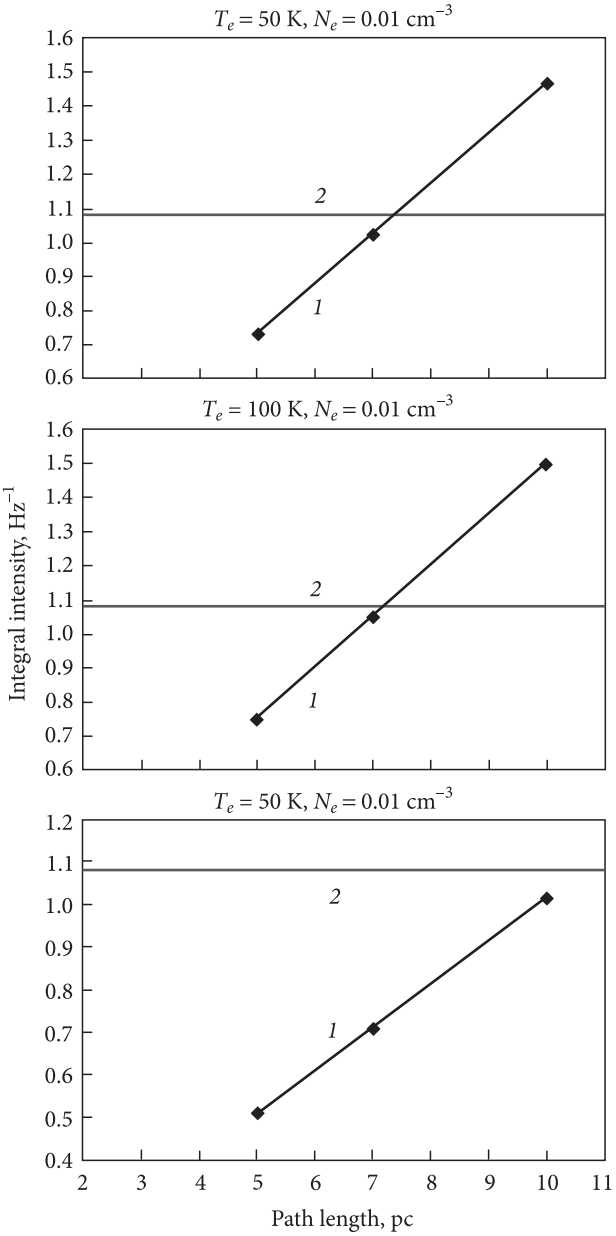

Fig. 1. Comparison of the integral line intensity calculated from Equation (1) at path lengths of 5, 7, and 10 pc (line *1*) and the observational results (line *2*) for the S140 direction. Hereinafter, the upper and the middle diagrams use $b_n\beta_n$ from [6], while the lower diagrams use $b_n\,\beta_n$ from [25]; the intensities are plotted with the opposite sign

$b_n\beta_n$ from [6] and combination (1) with $s = 10$ pc and $b_n\beta_n$ from [25] are preferable. For the G108.48+7.83, the preference is given to combinations (1) and (4) with $s = 7$ pc and $b_n\beta_n$ from [6] and to combination (1) with $s = 10$ pc and $b_n\beta_n$ from [25]. It can be seen that the RRLs originate from the regions with path lengths of 10 pc and even longer, which is quite expectable for a sight-line running in the Galactic plane where large volumes of interstellar gas reside. In the S140 direction, the present work identifies a basic radial velocity component, –16 km/s, and two weaker ones, –40 km/s and 7 km/s. The basic component is in general agreement with the measurements reported in [7—9], considering an approximately 1 kpc distance to the S140. The velocities –16 and 7 km/s obviously fit the local gas in the Orion arm. The velocity –40 km/s matches the gas that resides in the Perseus arm and whose component falls into the wide beam of the "North-South" array of the UTR-2.

Work [9] suggests that RRLs can form in various classes of ISM regions, including those directly related to the S140 nebula. The authors argue that in the local sight-line ISM, the line formation under the low-temperature dielectronic-like recombination mechanism seems less probable. To clarify the model of CII region, let us compare our decameter carbon RRL spectra to the HI line spectra synthesized within the angular resolution of the UTR-2 telescope in our studies of the S140, G105.15+2.8, and G108.48+7.83 directions. The spectra of both RRL types demonstrate a good agreement in respect of radial velocity, line width, and line intensity. For the G108.48+7.83 point in RRLs, the expected decay in line intensity is caused by this point deviation from the Galactic plane (relative to the G105.15+2.8 point). The decrease in line width is due to a smaller gas volume falling within the wide antenna beam. For HI line, these differences are also noticeable. Thus, we conclude that in this part of the Galaxy, large-scale HI cloud complexes extending up to the Galactic latitudes $b \sim +8°$ may exist. Consequently, decameter RRLs can most likely originate from the same gas as HI line, refuting the hypothesis from [9] that these lines form in small-size regions associated with the S140 nebula itself.

According to [10], the RRL widths measured at high and low frequencies in the S140 direction do not coincide, indicating that high-frequency and low-frequency lines may be from various medium regions. The CII regions responsible for the low-frequency line formation are apparently not directly related to the S140 nebula and to CII regions of the high-frequency line formation. That decameter carbon RRLs take place in the spectra plotted on the graphs in Figs 2 and 3 obtained in [1] for a medium region exceeding the S140 in angular size implies that the size of CII region or CII regions (in the S140 di-

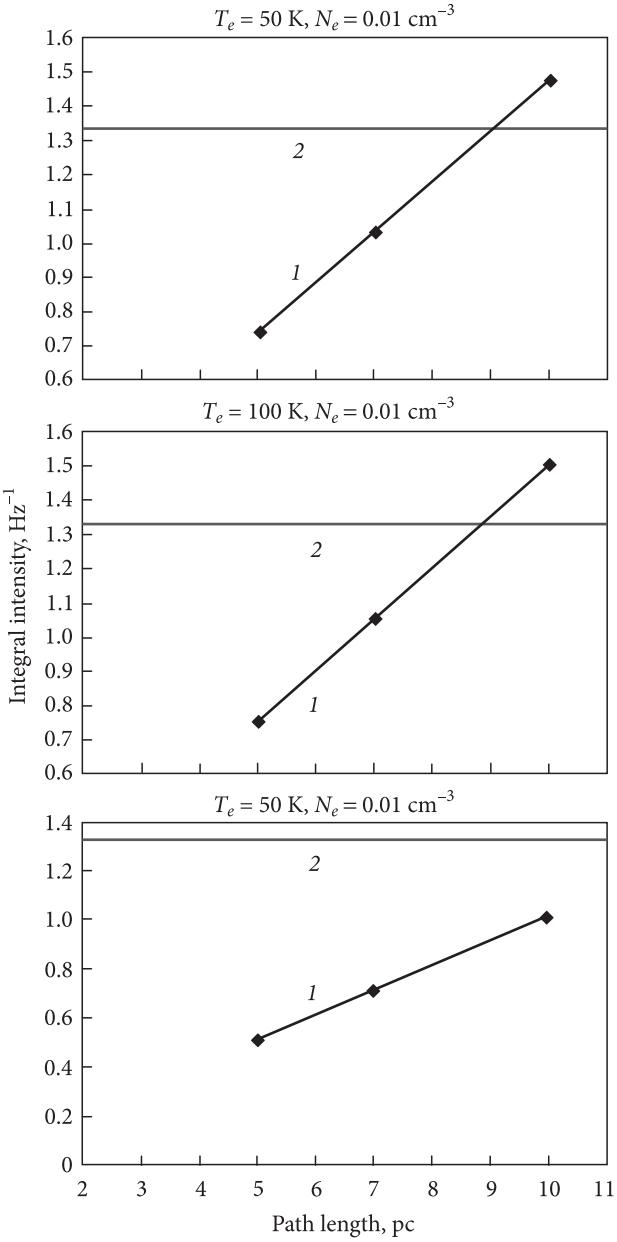

Fig. 2. Comparison of the model calculations of the integral line intensity (line *1*) and its observational values (line *2*) for the G105.15+2.8 direction

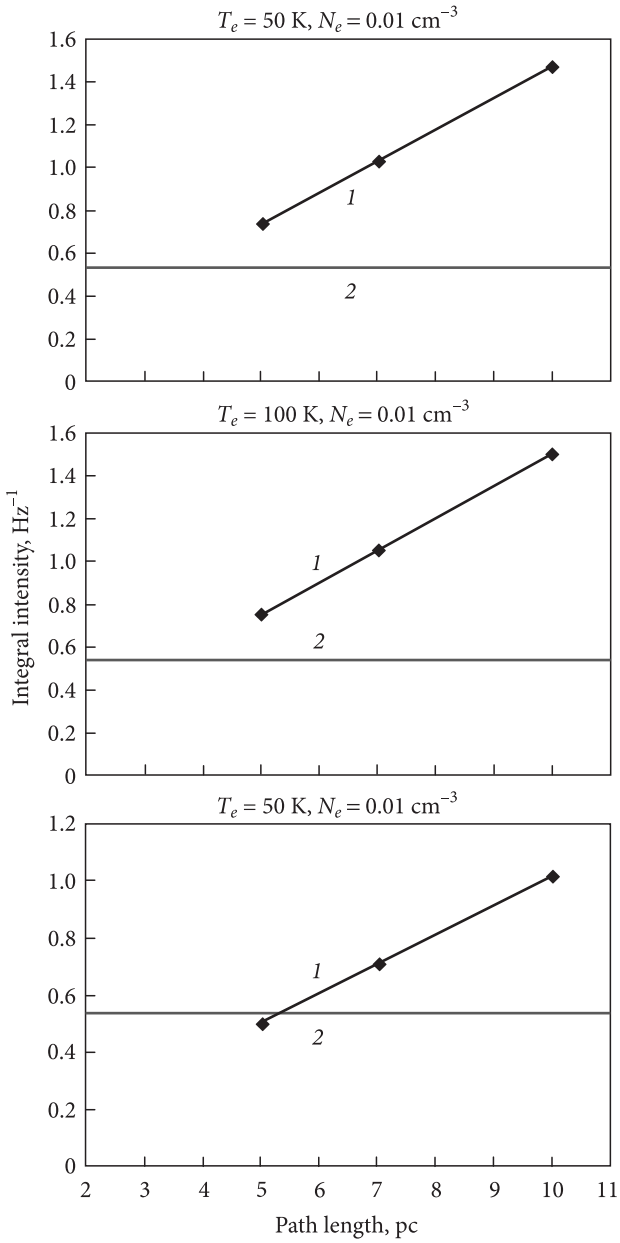

Fig. 3. Comparison of the model calculations of the integral line intensity (line *1*) and its observational values (line *2*) in the G108.48+7.83 direction

rection) responsible for the formation of these lines is larger than 6° by declination. Thus, the assumptions made in [10] are valid.

3. Analysis of physical conditions in the GSH 139-03-69 line of sight and its vicinity

The line widths in the GSH 139-03-69, G140+00, and G145+00 directions were determined by the Gaussian fitting into the observational spectra (see Table 2 in [1]). The radial velocities and the measured line widths in the GSH 139-03-69 direction do not differ much from those in the G145+00 and G140+00 directions. This gives grounds to believe that the observed RRLs in the case of the association of CII-regions and HI clouds track "ordinary" local HI gas omnipresent in the Galactic plane and not associated with extremely cold gas of the GSH 139-03-69 super shell. A comparison with the higher-frequency RRL widths in terms of radial velocities in the

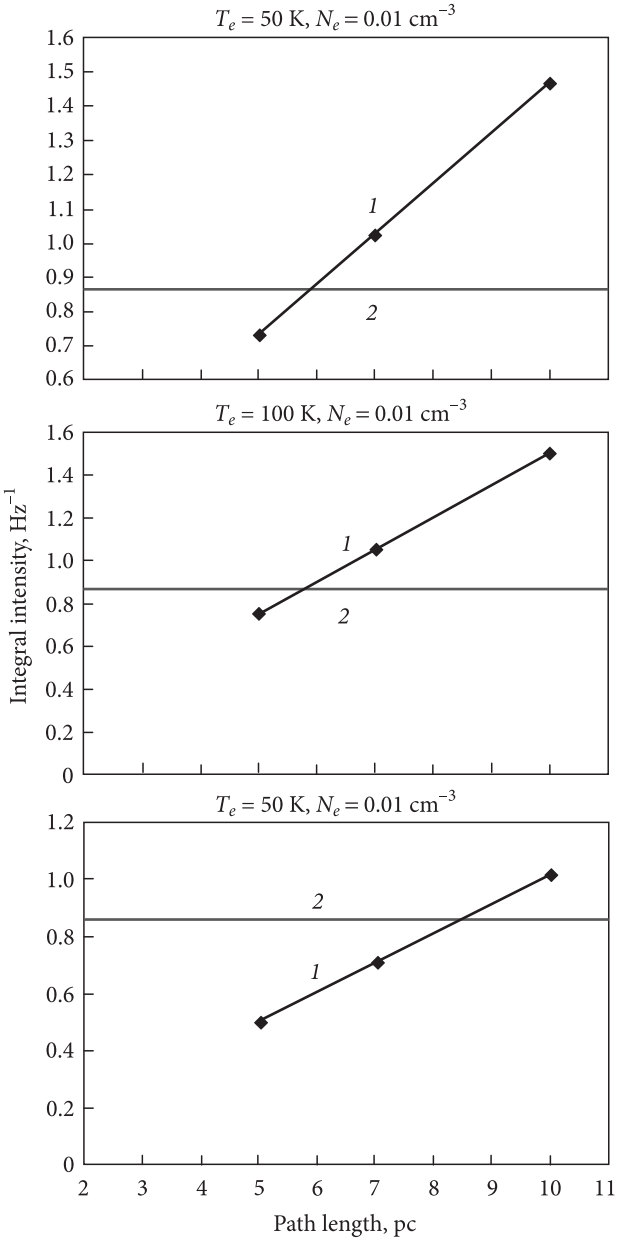

Fig. 4. Comparison of the model calculations of the integral line intensity (line *1*) and its observational values (line *2*) in the GSH 139-03-69 direction

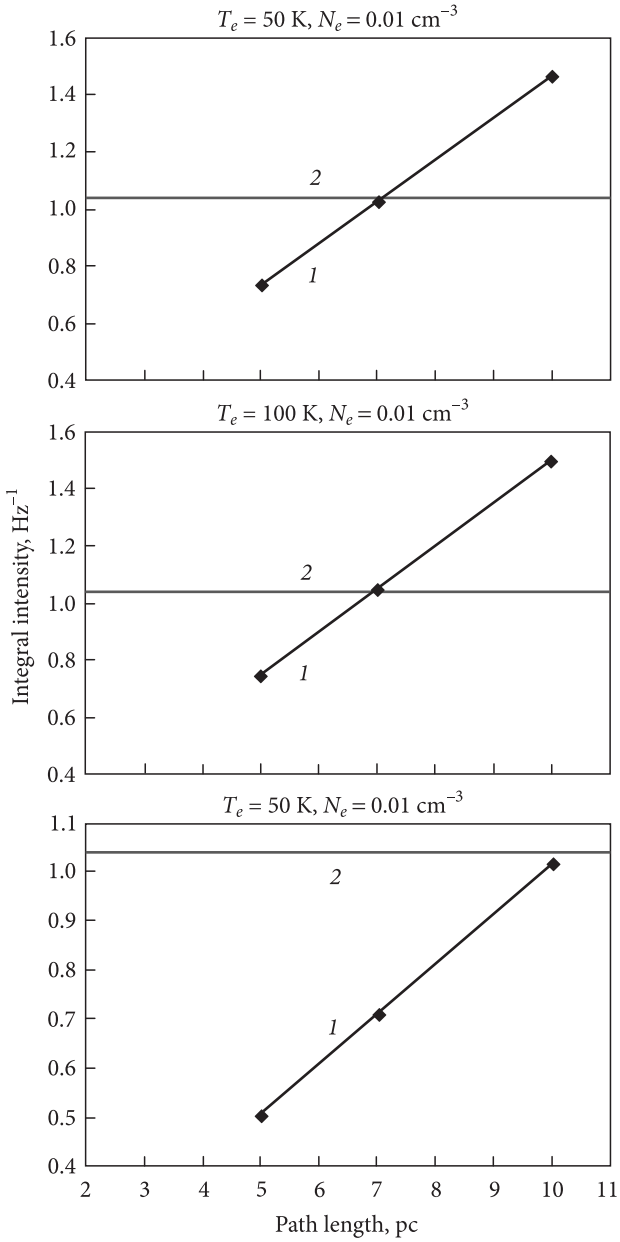

Fig. 5. Comparison of the model calculations of the integral line intensity (line *1*) and its observational values (line *2*) in the G140+00 direction

GSH 139-03-69 and nearby directions in the Galactic plane shows that low-frequency line widths are even somewhat smaller than high-frequency line widths. Hence, the Doppler broadening mechanism dominates.

For the GSH 139-03-69 direction, the spectrum shown in Fig. 5 in [1] has several line components whose radial velocities are approximately –32 and –7 km/s, suggesting that the gas traced by these components resides in the Perseus and Orion arms. In similar spectra taken a year later (Fig. 6, [1]), these two merge into one with a radial velocity of about –19 km/s, which can apparently be explained by a shorter accumulation time and, thus, a lower sensitivity. Furthermore, both spectra have a weaker and narrower component near –80 km/s. It corresponds to the radial velocities of the outer Galactic arm and is consistent with the observational results in [13]. This component is believed to match the absorption of the extremely cold gas in the GSH 139-03-69

super shell, but it is so faint that its detailed analysis and measurements of its characteristics require greater observational sensitivity.

The arc of the GSH 139-03-69 northern border at the point with coordinates $l = 145°$, $b = 0°$ was not defined well enough in the HI self-absorption line. In the spectrum presented in Fig. 7, [1], the RRLs are seen to have several components corresponding to radial velocities within –50÷0 km/s and associated with the gas in the Perseus and Orion spiral arms. The faint component which is barely visible near –80 km/s in Figs. 5 and 6 in [1] is missing. At the point with coordinates $l = 137°$, $b = –6°$, low-frequency carbon RRLs were not detected due to the lack of integration time (Fig. 8, [1]).

For the GSH 139-03-69, G140+00, and G145+00 directions, the iterative analysis of physical conditions most consistent with the experimental data was conducted with the use of Equation (1) by analogy with the analysis for the S140 direction. In the GSH 139-03-69 direction, the best correspondence to our data was obtained for combinations (1) and (4) with the path length $s = 5$ pc and $b_n\beta_n$ from [6] and for combination (1) with $s = 7$ pc and $b_n\beta_n$ from [25] (see Table 2, Fig. 4). For the G140+00 direction, the best correspondence is for combinations (1) and (4), with the path length $s = 7$ pc and $b_n\beta_n$ from [6] and for combination (1), $s = 10$ pc and $b_n\beta_n$ from [25] (Table 2, Fig. 5). For the G145+00 direction, the best correspondence is achieved for combinations (1) and (4), with the path length $s = 7$ pc and $b_n\beta_n$ from [6] and for combination (1), with $s = 10$ pc and $b_n\beta_n$ from [25] (Table 2, Fig. 6). Note that the observed radial velocities of the detected lines and their correlation with the corresponding HI spectra give reasons to conclude that the RRLs arise in local diffuse HI clouds in the Galactic plane and are not related to the GSH 139-03-69. The Sun is 9 kpc away from the GSH 139-03-69. The sensitivity of measurements is currently too low to examine the –80 km/s component associated with the absorption of the ionized gas in this super shell. The path lengths extracted from this direction analysis are slightly smaller than those in the neighboring G140+00 and G145+00 sight-lines. However, to draw any conclusions solely from this fact is premature since an analysis of physical conditions in this case only depends on the measured integral intensity alone. To obtain a more distinct and reliable picture, one should estimate the

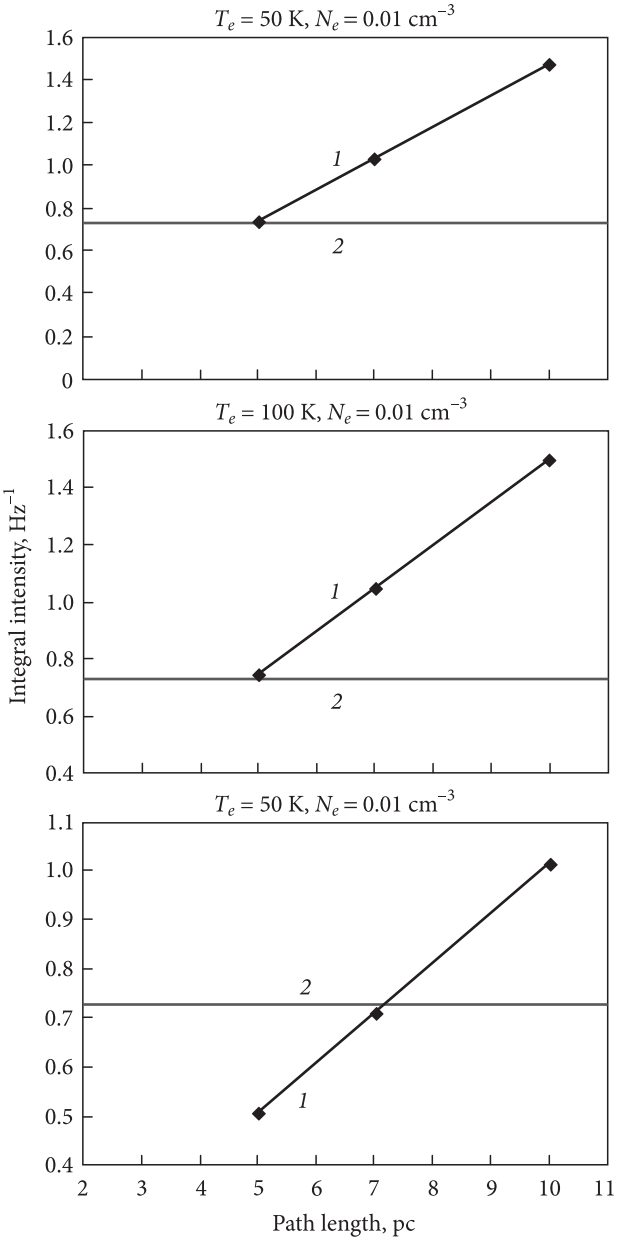

Fig. 6. Comparison of the model calculations of the integral line intensity (line *1*) and its observational values (line *2*) in the G145+00 direction

electron temperature and electron density (and, subsequently, the path length) and augment the stock of methods with multi-frequency observational techniques.

Only a piece of the complex border was observed in HI self-absorption line. Therefore, it makes sense to investigate the GSH 139-03-69 direction and its vicinity with a high spatial resolution and a good sensitivity by means of low-frequency RRL scanning of areas of the size $l \times b = 18° \times 10°$ with the center in

the GSH 139-03-69 sight-line. Also, all available data in HI self-absorption line in these directions should be used. The fact that decameter carbon RRLs can distinguish between hot and cold gas with great accuracy, which is almost impossible by observations in HI line, confirms that we will be able to track the border, estimate the size of the object, and gain more insight into its physics.

Conclusions

Part 2 of the current paper has contributed to the understanding of the physical conditions in CII regions that produce decameter carbon RRLs viewed near the frequency 26 MHz through the UTR-2 radio telescope towards the S140 emission nebula and the GSH 139-03-69 super shell.

In Part 1 of the current paper, we concluded that CII region responsible for decameter carbon line formation in the S140 direction is not associated with the S140 nebula itself. The line characteristics in both the S140 sight-line and its vicinity are very similar, suggesting that CII region is rather extended (more than 6° by declination) and that the RRLs may form in such widespread ISM components as HI clouds in the Galactic plane. A comparison between ionized carbon and HI spatial distributions validates this assumption. Of the existing CII region models, our data best fall within the "warm" model of line formation regions, with ionized carbon thought of as associated with diffuse HI clouds at $T_e \sim 35 \div 75$ K and $N_e \sim 0.05 \div 0.1$ cm^{-3}. The iterative comparison of detected and model integral intensities of decameter carbon RRLs for different T_e, N_e, and s combinations yielded the physical state ranges where observational data and model predictions are in the best agreement. The best coincidence with our data was found for the combination $T_e = 50 \div 100$ K, $N_e = 0.01$ cm^{-3}, and $s = 10$ pc. Furthermore, the model computation of integral intensities involved new, more precise values of the departure coefficients $b_n\beta_n$.

For the GSH 139-03-69 line of sight, the physical condition of the local ISM gas has been estimated, too, offering $T_e = 50 \div 100$ K, $N_e = 0.01$ cm^{-3}, and $s = 5 \div 7$ pc. The decameter carbon RRLs most likely originate from the local HI that resides in the Galactic plane. The spectral component responsible for the gas absorption in the super shell itself is too faint to admit its proper analysis today.

However, it should be noted that due to the absence of a strong discrete continuum source such that its brightness temperature exceeds the Galactic background temperature we need to know the spatial structure of CII regions in given directions to faithfully determine the medium parameters and interpret them properly. Also, for estimating physical conditions in the ISM gas, the stock of employed research methods is necessary to be augmented with multi-frequency observational techniques.

This work was performed with the support of the Targeted Comprehensive Program of the National Academy of Sciences of Ukraine "Development of domestic radio astronomy and its integration into modern global research radio networks of the Universe" for 2018—2022 (0118U000561, 0119U101514, 0120U101479, 0121U109280, 0122U002537); the Targeted Comprehensive Program of the National Academy of Sciences of Ukraine "Support of priority state of scientific research and scientific and technical (experimental) developments of Physics and Astronomy Department of the National Academy of Sciences of Ukraine" for 2022. (0123U102426) as well as departmental research program 0122U000793.

REFERENCES

1. Vasylkivskyi, Y.V., Konovalenko, O.O., Stepkin, S.V., 2023. Observations of decameter carbon radio recombination lines toward several Galactic directions. Part 1. Experimental study. *Radio Phys. Radio Astron.,* **28**(3), pp. 201—211. DOI: 10.15407/rpra28.03.201
2. Konovalenko, A.A., and Sodin, L.G., 1981. The 26.13 MHz absorption line in the direction of Cassiopeia A. *Nature,* **294**, pp. 135—136. DOI: 10.1038/294135a0
3. Gordon, M.A., and Sorochenko, R.L., 2009. *Radio Recombination Lines. Their Physics and Astronomical Applications*. Ser. Astrophysics and Space Science Library. Vol. 282. New York: Springer Science + Business Media. DOI: 10.1007/978-94-010-0261-5
4. Konovalenko, A.A., and Stepkin, S.V., 2005. Radio Recombination Lines. In: L.I. Gurvits, S. Frey, and S. Rawlings, eds., *Radio Astronomy from Karl Jansky to Microjansky.* Budapest, Hungary: EAS Publ., **15**, pp. 271—295. DOI: 10.1051/eas:2005158

5. Stepkin, S.V., Konovalenko, O.O., Vasylkivskyi, Y.V., Mukha, D.V., 2021. Interstellar medium and decameter radio spectroscopy. *Radio Phys. Radio Astron.,* **26**(4), pp. 314—325. DOI: 10.15407/rpra26.04.314
6. Walmsley, C.M., and Watson, W.D., 1982. The influence of dielectronic-like recombination at low temperatures on the interpretation of interstellar, radio recombination lines of carbon. *Astrophys. J.,* **260**, pp. 317—325. DOI: 10.1086/160256
7. Knapp, G.R., Brown, R.L., Kuiper, T.B.H., Kaakr, R.K., 1976. Carbon recombination line observations of the sharpless 140 region. *Astrophys. J.,* **204**(1), pp. 781—783. DOI: 10.1086/154225
8. Smirnov, G.T., Sorochenko, R.L., Walmsley, C.M., 1995. The S 140/L 1204 complex: radio recombination lines of hydrogen, carbon and sulphur. *Astron. Astrophys.,* **300**, pp. 923—932.
9. Golynkin, A.A., Konovalenko, A.A., 1991. Radio recombination lines of highly excited carbon near DR21 and S140. *Sov. Astron. Lett.,* **16(**1), pp. 7—10.
10. Smirnov, G.T., Sorochenko, R.L., Kitaev, V.V., 1992. Search for 42 MHz recombination lines toward S140. *Sov. Astron. Lett.,* **18**, pp. 192—194.
11. Vasylkivskyi, Y.V., Stepkin, S.V., Konovalenko, O.O., 2023. Studies of low-frequency carbon radio recombination lines in medium toward S140 nebula. *Contr. Astr. Obs. Skalnate Pleso*, **53**(1), pp. 17—27. DOI: 10.31577/caosp.2023.53.1.17
12. Kalberla, P.M.W., Burton, W.B., Hartman, Dap, Arnal, E.M., Bajaja, E., Morras, R., Pöppel, W.G.L., 2005. The Leiden/Argentine/Bonn (LAB) survey of Galactic HI: final data release of the combined LDS and IAR surveys with improved stray-radiation corrections. *Astron. Astrophys.,* **440**(2), pp. 775—782. DOI: 10.1051/0004-6361:20041864
13. Knee, L.B.G., Brunt, C.M., 2001. A massive cloud of cold atomic hydrogen in the outer Galaxy. *Nature,* **412**, pp. 308—310. DOI: 10.1038/35085519
14. Ershov, A.A., Ilyashov, Y.P., Lekht, E.E., Smirnov, G.T., Solodkov, V.T., Sorochenko, R.L., 1984. Low-frequency (42, 57, 84 MHz) excited-carbon lines toward Cassiopeia A. *Sov. Astron. Lett.,* **10**, pp. 348—353.
15. Konovalenko, A.A., 1984. Observations of carbon recombination lines at decametric wavelengths in the direction Cassiopeia A. *Sov. Astron. Lett.,* **10**, pp. 353—356.
16. Ershov, A.A., Lekht, E.E., Smirnov, G.T., Sorochenko, R.L., 1987. Highly excited-carbon level population and nature of the low-frequency radio line forming regions toward Cassiopeia A. *Sov. Astron. Lett.,* **13**, pp. 8—11.
17. Payne, H.E., Anantharamaiah, K.R., Erickson, W.C., 1989. Stimulated emission of carbon recombination lines from cold clouds in the direction of Cassiopeia A. *Astrophys. J.,* **341**, pp. 890—900. DOI: 10.1086/167547
18. Payne, H.E., Anantharamaiah, K.R., Erickson, W.C., 1994. High Rydberg state carbon recombination lines toward Cassiopeia A: Physical conditions and a new class of models. *Astrophys. J.,* **430**, pp. 690—705. DOI: 10.1086/174441
19. Sorochenko, R.L., 1996. Radio recombination lines as a tool for investigation of molecular clouds. *Astron. Astrophys. Trans.,* **11**(3), pp. 199—214. DOI: 10.1080/10556799608205467
20. Kantharia, N.G., Anantharamaiah, K.R., and Payne, H.E., 1998. Carbon Recombination Lines between 34.5 and 770 MHz toward Cassiopeia A. *Astrophys. J.,* **506**(2), pp. 758—772. DOI: 10.1086/306266
21. Oonk, J.B.R., van Weeren, R.J., Salas, P., Salgado, F., Morabito, L.K., Toribio, M.C., Tielens, A.G.G.M., Röttgering, H.J.A., 2016. Carbon and hydrogen radio recombination lines from the cold clouds towards Cassiopeia A. *Mon. Not. R. Astron. Soc.,* **465**(1), pp. 1066—1088. DOI: 10.1093/mnras/stw2818
22. Salas, P., Oonk, J.B.R., van Weeren, R.J., Salgado, F., Morabito, L.K., Toribio, M.C., Emig, K., Röttgering, H.J.A., and Tielens, A.G.G.M., 2017. LOFAR observations of decameter carbon radio recombination lines towards Cassiopeia A. *Mon. Not. R. Astron. Soc.,* **467**(2), pp. 2274—2287. DOI: 10.1093/mnras/stx239
23. Erickson, W.C., McConnell, D., Anantharamaiah, K.R., 1995. Low-frequency carbon recombination lines in the central regions of the Galaxy. *Astrophys. J.,* **454**, pp. 125—133. DOI: 10.1086/176471
24. Kantharia, N.G., Anantharamaiah, K.R., 2001. Carbon recombination lines from the Galactic plane at 34.5 & 328 MHz. *J. Astrophys. Astron.,* **22**, pp. 51—80. DOI: 10.1007/BF02933590
25. Salgado, F., Morabito, L.K., Oonk, J.B.R., Salas, P., Toribio, M.C., Röttgering, H.J.A., and Tielens, A.G.G.M., 2017. Low-frequency carbon radio recombination lines. I. Calculation of departure coefficients. *Astrophys. J.,* **837**(2), id. 141. DOI: 10.3847/1538-4357/aa5d9e

Received 03.03.2023

Є.В. Васильківський, О.О. Коноваленко, С.В. Степкін

Радіоастрономічний інститут НАН України
вул. Мистецтв, 4, м. Харків, 61002, Україна
E-mail: vasylkivskyi@rian.kharkov.ua

СПОСТЕРЕЖЕННЯ ДЕКАМЕТРОВИХ РЕКОМБІНАЦІЙНИХ
РАДІОЛІНІЙ ВУГЛЕЦЮ В ДЕЯКИХ НАПРЯМКАХ ГАЛАКТИКИ
Частина 2. АНАЛІЗ ФІЗИЧНИХ УМОВ У ДИФУЗНИХ CII-ОБЛАСТЯХ

Предмет і мета роботи. У цій статті описано аналіз результатів спостережень декаметрових рекомбінаційних радіоліній (РРЛ) вуглецю, виконаних у напрямках емісійної туманності S140 і гігантської оболонки GSH 139-03-69 на радіотелескопі УТР-2 поблизу частоти 26 МГц. Такі лінії є високоефективним засобом діагностики холодного розрідженого міжзоряного

середовища (МЗС). Метою даної роботи є визначення зв'язку областей формування цих декаметрових ліній (СІІ-областей) з іншими компонентами МЗС, а також дослідження фізичних умов у цих областях (електронна температура T_e, електронна густина N_e).

Методи та методологія. Шляхом ітераційного порівняння експериментально отриманих інтегральних інтенсивностей декаметрових РРЛ вуглецю з їхніми модельними значеннями для різних комбінацій T_e, N_e, а також розміру області крізь промінь зору s, було визначено діапазони фізичних умов, для яких спостерігається найкраще узгодження.

Результати. Характеристики зареєстрованих декаметрових РРЛ вуглецю узгоджуються з більш високочастотними даними як для напрямку S140, так і для інших напрямків Галактичної площини, в тому числі й поблизу GSH 139-03-69. Було визначено діапазони фізичних умов, для яких найкращим чином узгоджуються експериментальні та модельні дані. Для напрямку на туманність S140 та її околиці найкраще узгодження спостерігається для $T_e = 50…100$ К, $N_e = 0.01$ см$^{-3}$ та $s = 10$ пк. Для напрямку на оболонку GSH 139-03-69 найкраще узгодження відповідає $T_e = 50…100$ К, $N_e = 0.01$ см$^{-3}$ та $s = 5…7$ пк.

Висновки. Отримані результати свідчать про те, що зареєстровані декаметрові РРЛ вуглецю утворились у СІІ-областях, асоційованих із хмарами дифузного нейтрального водню HI в Галактичній площині. Лінії утворилися на тлі фонового Галактичного радіовипромінювання, яскравісна температура якого зростає зі зменшенням частоти.

Ключові слова: *електронна густина, електронна температура, іонізований вуглець, міжзоряне середовище, модель середовища, рекомбінаційні радіолінії, СІІ-область.*